Journal of the Mechanical Behavior of Biomedical Materials 98 (2019) 40–47

Contents lists available at ScienceDirect

Journal of the Mechanical Behavior of Biomedical Materials

journal homepage: www.elsevier.com/locate/jmbbm

Combined wear and ageing of ceramic-on-ceramic bearings in total hip replacement under edge loading conditions

Mazen Al-Hajjar[a], Laurent Gremillard[b], Sabine Begand[c,e], Thomas Oberbach[c], Karen Hans[c], Daniel Delfosse[d], Jérôme Chevalier[b], Louise M. Jennings[a,*]

[a] Institute of Medical and Biological Engineering, School of Mechanical Engineering, University of Leeds, Leeds, UK
[b] Univ Lyon, INSA Lyon, CNRS, MATEIS UMR, 5510, Bât. Blaise Pascal, 7 Avenue Jean Capelle, Villeurbanne, France
[c] Mathys Orthopädie GmbH, Moersdorf, Germany
[d] Mathys AG Bettlach, Switzerland
[e] Fraunhofer IKTS, Hermsdorf, Germany

ARTICLE INFO

Keywords:
Ceramic on ceramic
Hip replacement
Stripe wear
Edge loading
Hydrothermal ageing

ABSTRACT

Ceramic-on-ceramic bearings in total hip replacement have shown the potential to provide low wear solutions in hip replacement. Assessing the tribological performance of these materials is important to predict their long-term performance in patients. In this study, a methodology was devised to assess the tribological *in vitro* behaviour of composite ceramics under combined adverse edge loading conditions and accelerated ageing. Two commercial ceramic composites were considered, namely Alumina-Toughened Zirconia (ATZ, ceramys®) and Zirconia-Toughened Alumina (ZTA, symarec®). The bearing couples were studied using the Leeds Mark II hip joint simulator for a total of eight million cycles, the first two million under normal gait (no edge loading) and the following six million cycles with the addition of edge loading conditions driven by medial-lateral separation. The bearing couples underwent hydrothermal ageing using an accelerated protocol in autoclave every million cycles.

The influence of edge loading combined with ageing was significant for ATZ bearings, resulting in a slower overall ageing kinetics over the wear stripe than on the control heads. During the autoclave ageing steps, the monoclinic fraction increased more over the wear stripe area than over the unworn area. Both results thus indicated that the monoclinic phase was removed during shocks induced by edge loading. The wear performance of the two materials were similar exhibiting relatively low wear rates and low level of microstructural damage for these clinically relevant adverse conditions.

1. Introduction

Ceramic-on-ceramic (CoC) bearings for total hip replacement have been used as alternatives to metal-on-polyethylene (MoP) bearings due to their superior tribological properties (Bierbaum et al., 2002). They were introduced by Boutin in the early 1970s (Boutin, 1971). The wear of CoC bearings is very low under standard gait conditions (Al-Hajjar et al., 2010). Ceramic materials in hip replacement have evolved significantly from pure Alumina since they were introduced. Currently, widely used ceramic materials are composites, mostly a mixture of alumina and zirconia. These composite materials have shown better tribological and mechanical properties than the pure alumina ceramics (Sentuerk et al., 2016). Prospective clinical studies have shown the advantages of using CoC bearings in younger patients, with cumulative rate of survival of 99% at 10 years (D'Antonio et al., 2012) and 84.4% at 20 years (Petsatodis et al., 2010).

Since most current composite CoC bearings are zirconia-based, hydrothermal ageing of zirconia can be a concern (Kobayashi et al., 1981). This phenomenon occurs when the surface of zirconia-containing materials is exposed to water and, moreover, may be accelerated by friction (Gremillard et al., 2013). Both conditions are pertinent to CoC orthopaedic prostheses. Hydrothermal ageing is the result of a phase transformation, from the metastable, tetragonal zirconia phase to the stable monoclinic one (t-m transformation). Thus, it is quantified following the evolution of the proportion of monoclinic phase with time. Since the t-m transformation is accompanied by a 4-to-5 vol. % increase, it usually results in an increase of the roughness (due to transformed grains protruding from the surface). Since the limited plasticity of ceramics prevents the accommodation of this volume increase, microcracking may take place on the surface. Microcracking has been

* Corresponding author.
E-mail address: l.m.jennings@leeds.ac.uk (L.M. Jennings).

https://doi.org/10.1016/j.jmbbm.2019.05.011
Received 15 January 2019; Received in revised form 15 April 2019; Accepted 6 May 2019
Available online 18 May 2019

shown to be more extensive in zirconia than in alumina-toughened zirconia (zirconia matrix with alumina as the second phase) (Gremillard et al., 2018). It is almost not existent in zirconia-toughened alumina (alumina matrix with zirconia as a second phase), where ageing is slower and concerns a minority of the total material (Gremillard et al., 2018).

Previous studies have shown the importance of replicating edge loading conditions in pre-clinical testing due to separation between the femoral head and acetabular cup (Nevelos et al., 2000; Stewart et al., 2003a, 2003b; Leslie et al., 2009). Clinically, edge loading may occur due to many factors, including implant design, implant positioning, patient's anatomy and biomechanics. For example, in a recent case report of fracture of a ceramic composite liner without history of trauma in a well-fixed total hip implant, the authors found signs of stripe wear on the inner surface of the ceramic liner, leading them to believe the possible cause of fracture in this patient was edge loading due to joint laxity (Yoon and Park, 2018). Fluoroscopy studies have shown that separation of centres of rotation of the head and cup occurs during gait (Blumenfeld et al., 2011; Dennis et al., 2001) hence leading to adverse mechanical and tribological conditions. The wear rate of ceramic-on-ceramic bearings was reported to increase under edge loading conditions *in vitro* to levels similar to those observed *in vivo* (Al-Hajjar et al., 2010; Nevelos et al., 2000; Stewart et al., 2003a). This method can differentiate between the performances of different ceramic-on-ceramic materials under clinically relevant adverse conditions (Stewart et al., 2003b; Al-Hajjar et al., 2013a, 2017).

It is thus important to evaluate new ceramic-on-ceramic material under clinically relevant conditions representing adverse conditions experienced by the prostheses in patients and also taking into consideration the potential biomaterial degradation changes these prostheses go through during their use in patients. The aim of this study was to determine the wear rates, phase transformation and wear mechanisms of CoC bearings made of alumina-toughened zirconia (ATZ-on-ATZ) and zirconia-toughened alumina (ZTA-on-ZTA) under standard gait and edge loading conditions combined with hydrothermal ageing.

2. Materials and methods

Femoral heads and acetabular liners of hip prostheses were provided by Mathys Ltd Bettlach and made of two materials: Alumina-Toughened Zirconia (ATZ, ceramys®, composed of 80 wt% 3 Y-TZP (3 mol.% Yttria Stabilized Tetragonal Zirconia Polycrystal) and 20 wt% α-Al_2O_3, *i.e.* 72.4 and 27.6 vol% respectively) and zirconia-toughened alumina (ZTA, symarec®, composed of 75 wt% α-Al_2O_3 and 25 wt% 3 Y-TZP, *i.e.* 82 and 18 vol% respectively). Rietveld refinement of flat ATZ and ZTA disks provided by Mathys Ltd Bettlach confirmed the α-Al_2O_3 content by weight to be 20% and 73% respectively. It was not possible to fully confirm the phase composition of the hip components since the non-flat geometry gives rise to too many artefacts for Rietveld refinement. Two material combinations were tested in this study: ATZ femoral head with ATZ acetabular liner (ATZ-on-ATZ) and ZTA femoral head with ZTA acetabular liner (ZTA-on-ZTA). All components were sterilized by gamma radiation (Co-60 source, radiation dose between 25 and 45 kGy) before the testing protocol.

A total of six bearing couples were studied on the Leeds Mark II Physiological Anatomical hip joint simulator (Fig. 2). Three bearing couples were tested for each material combination with a femoral head diameter of 32 mm. The femoral head was taper-locked onto a femoral hip stem mounted in acrylic cement. The acetabular liner was held in a metallic shell which was mounted in the cup holder at an angle of 45° which is equivalent to 55° *in vivo* (Williams et al., 2008). Alignment marks were engraved on all components to ensure accurate re-positioning of implant after each measurement point.

The study process is shown in Fig. 1 and this was repeated eight times; two million cycles under standard conditions and six million cycles under edge loading conditions. Hence the study was run for a total of eight million cycles. The first two million cycles were run using standard gait conditions (Barbour et al., 1999) and the subsequent 6 million cycles were run under edge loading conditions due to dynamic separation between the femoral head and the acetabular cup. The simulator was run using a physiological walking cycle with a twin peak time dependent loading curve and an elliptical wear path at a frequency of 1 Hz. The flexion/extension was +30°/-15° applied to the femoral head and internal/external rotation was ± 10° applied to the acetabular cup. A twin peak Paul type loading curve was applied with a peak load of 3 kN and swing phase load of 300 N. The dynamic separation (causing edge loading conditions) was achieved by applying a lateral to medial load to the acetabular cup using springs (Fig. 2). This produced medial and superior translation of the acetabular cup relative to the femoral head during the swing phase of the simulator cycle. The spring force was adjusted manually to produce a separation of approximately 500 µm, with a reduced swing phase load (~70 N). The separation was monitored throughout the test using a calibrated Linear Variable Differential Transformer (LVDT) position sensor.

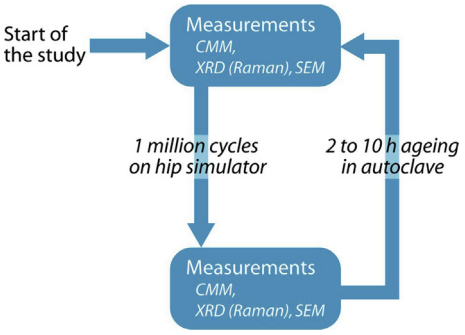

Fig. 1. Flow chart showing the process followed when conducting the study. This was repeated eight times; two million cycles under standard conditions and six million cycles under edge loading conditions.

All femoral heads and acetabular cups were hydrothermally aged during the wear study after every million cycles of testing. The hydrothermal ageing of components started after the components were tested for one million cycles under standard conditions on the hip joint simulator. It lasted 2 h at 134 °C after each million cycles until 3 million cycles representing few years *in vivo*. After the 4th million cycles it was discovered that the time-temperature equivalence for hydrothermal ageing was not the same in ATZ and ZTA. Thus, so as not to risk an underestimation of the effects of ageing, it was decided to lengthen the ageing steps to 10 h after each million cycles. To distinguish the effects

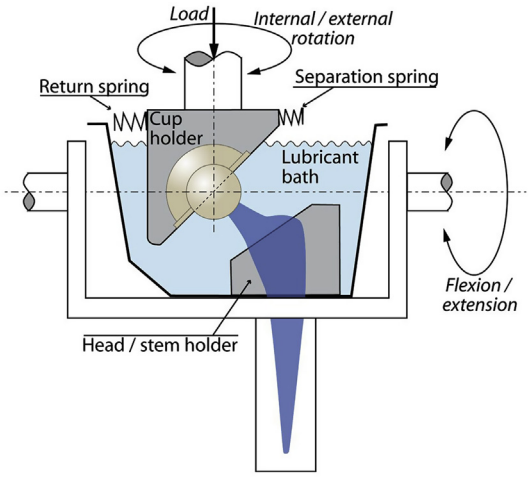

Fig. 2. Schematic of one station of the Leeds Mark II Physiological Anatomical hip joint simulator.

of ageing from those of wear and edge loading, 3 heads for each material (control heads) were also aged with the same ageing conditions but without being tested in the hip joint simulator. Hydrothermal ageing was achieved using a ccelerated ageing protocol in an autoclave (Sanoclav LA-MCS, Wolf, Germany) in water vapour. Since hydrothermal ageing is thermally activated (following an Arhenius law), it is possible to simulate the hydrothermal ageing taking place over a few years at body temperature by accelerated ageing protocols at higher temperature, following equation (1) (expressing that the monoclinic fraction is the same at both time-temperature couples (t_1,T_1) and (t_2,T_2), Q being the activation energy of ageing and R the gas constant).

$$t_2 = t_1 \exp\left[\frac{Q}{R}\left(\frac{1}{T_2} - \frac{1}{T_1}\right)\right] \quad \text{(Eq. 1)}$$

Hydrothermal ageing kinetics were characterized using X-ray diffraction, with a D8-advance diffractometer (Bruker, Germany) equipped with a LynxEye Position Sensitive Detector, using Cu K_α radiations. Scans were performed between 26° and 33° (2θ), with a 0.02° step and a 0.3 s/step scan rate. Every head was measured at least in two locations: an area away from the wear stripe and over the wear stripe formed as a result of edge loading.

The volume monoclinic fraction was determined using Garvie and Nicholson's equation (Garvie and Nicholson, 1972) modified by Toraya (Toraya et al., 1984) (Eq. (2), in which X_m is an intensity ratio, and I^p_{hkl} denotes the integrated intensity of the peak related to the reticular planes *(hkl)* in the phase *p* (monoclinic, m, or tetragonal, t)).

$$V_m = \frac{1.311X_m}{1 + 0.311X_m} \quad \text{(Eq. 2-a)}$$

With

$$X_m = \frac{I^m_{111} + I^m_{111}}{I^m_{111} + I^m_{111} + I^t_{101}} \quad \text{(Eq. 2-b)}$$

After 6 M cycles and 26 h of ageing (with a missing point at 7 M cycles and 36 h, between wear testing and ageing), the characterization of aged specimens was also conducted using confocal Raman microscopy (Labram HR800 Evolution (Horiba - Jobin Yvon) with a 532 nm laser excitation). In particular, at selected times the thickness of the transformed, monoclinic layer was determined: Z-scans were conducted from 10 µm below the surface to 10 µm above it. At each Z position the monoclinic content was determined using Clarke and Adar's equation (Eq. (3) (Clarke and Adar, 1982). The obtained monoclinic profile was then fitted by a Cauchy function, the full width at half maximum of this function being considered as the thickness of the monoclinic layer. In addition, composition maps were obtained across the edge-loading zone. In these maps, the monoclinic fraction V_m was obtained using again Clarke and Adar's equation. However, to our knowledge no such equation exists for the determination of alumina content, thus the alumina fraction was deemed as varying in the same way as a simple intensity ratio (V_A) between alumina and zirconia peaks (Eq. (4). Note that V_A should not be used to quantify the alumina fraction, but only to characterize its variations during the tests.

$$V_m = \frac{I^{178}_m + I^{189}_m}{0.97(I^{145}_t + I^{260}_t) + I^{178}_m + I^{189}_m} \quad \text{(Eq. 3)}$$

$$V_A = \frac{I^{405}_A}{I^{145}_t + I^{260}_t + I^{178}_m + I^{189}_m} \quad \text{(Eq. 4)}$$

Scanning Electron Microscopy observations were conducted on pristine, worn and aged surfaces on the heads after various testing times, using a Supra 55 VP microscope (Zeiss, Germany), at low acceleration voltage (1–2 kV) so as to avoid coating the observed surfaces.

The wear was measured gravimetrically using a balance (XP205, Mettler-Toledo) at an interval of one million cycles. A coordinate measuring machine (Legex 322, Mitutoyo, Japan) was used to reconstruct the surface of the femoral head and acetabular cup. This machine had a 0.8 µm resolution. A 3 mm stylus was used with a vertical probe configuration. All femoral heads were measured by taking 72 traces over the femoral heads surfaces with 5° spacing about the vertical axis. Each trace started at the pole of the component and had a 0.2 mm pitch. The acetabular cups were measured by taking points in the form of 72 traces rotated by 5° from each other about the vertical axis. Each trace consisted of points with a pitch of 0.2 mm starting at the pole and finishing at the rim of the cup. RedLux software (RedLux, UK) was used to visualise the size, shape and penetration depth of the wear areas. The mean and 95% confidence limits were determined for the wear rates and penetration depths. One-way ANOVA was used to compare between means and significance was taken at $p < 0.05$.

The data associated with this article is openly available through the University of Leeds Data repository (Al-Hajjar and Jennings, 2019).

3. Results

The wear rates of both aged materials, ATZ-on-ATZ and ZTA-on-ZTA, under standard conditions were very low, i.e. < 0.01 mm^3/million cycles. There was no measurable change in the wear rate due to ageing under standard conditions.

The wear rates increased when edge loading conditions driven by separation was introduced to the gait cycle (Fig. 3). The mean wear rate of aged ZTA-on-ZTA after six million cycles of testing under edge loading conditions was 0.19 ± 0.47 mm^3/million cycles. This was 2.8-fold higher than the mean wear rate of aged ATZ-on-ATZ which was 0.07 ± 0.05 mm^3/million cycles. The difference was not statistically significant (p = 0.38) due to high variations in wear of ZTA-on-ZTA. In fact, one ZTA-on-ZTA couple (ZTA-on-ZTA 3 in Fig. 3) had a wear rate of 0.41 mm^3/million cycles over the six million cycles of test under edge loading compared to 0.07 mm^3/million cycles and 0.09 mm^3/million cycles for the other two couples. This high wearing couple experienced high wear rate between 3 and 4 million cycles of test of 0.74 mm^3/million cycles with higher penetration depth. Throughout the test, the amount of wear was split approximately 50:50 between the femoral head and the acetabular liner for all bearing couples.

There was no visible damage on the surfaces of the femoral head and acetabular cup after testing under standard conditions. In contrast, under edge loading conditions, a stripe-like wear area was observed on the femoral head with corresponding wear on the rim of the acetabular liner (Fig. 4). The penetration depths on the femoral heads and acetabular liners of the ZTA-on-ZTA bearings were higher than that of the

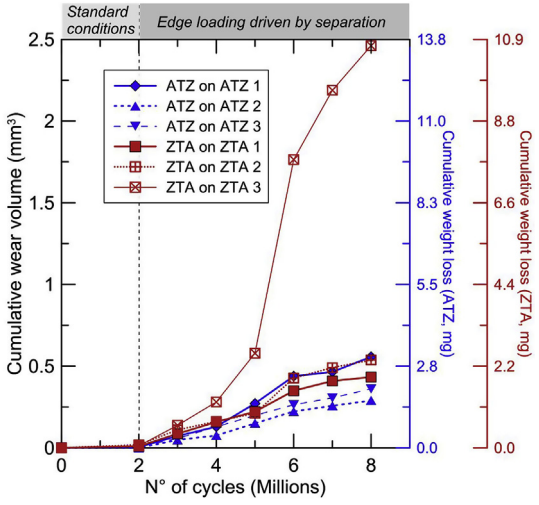

Fig. 3. Cumulative wear volume of ATZ-on-ATZ and ZTA-on-ZTA bearings over eight million cycles of hip simulator testing (first 2 million cycles in standard conditions, next 6 million in edge loading conditions driven by separation).

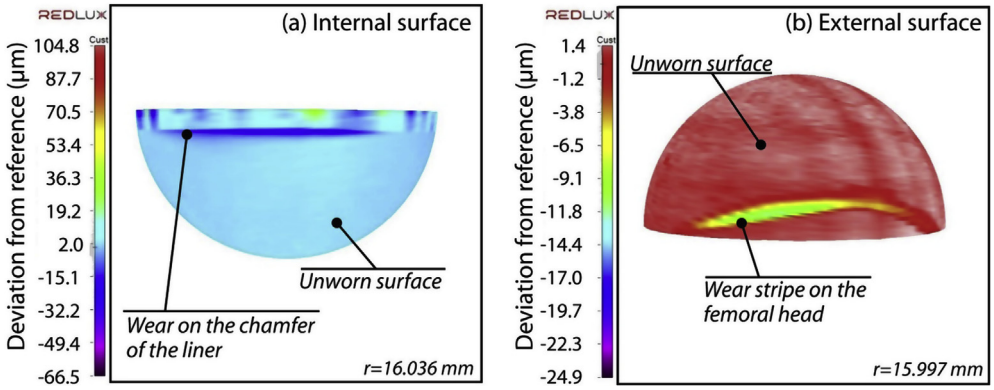

Fig. 4. Three-dimensional representation of the wear scar area on the acetabular liner (a) and femoral head (b) obtained using the RedLux software.

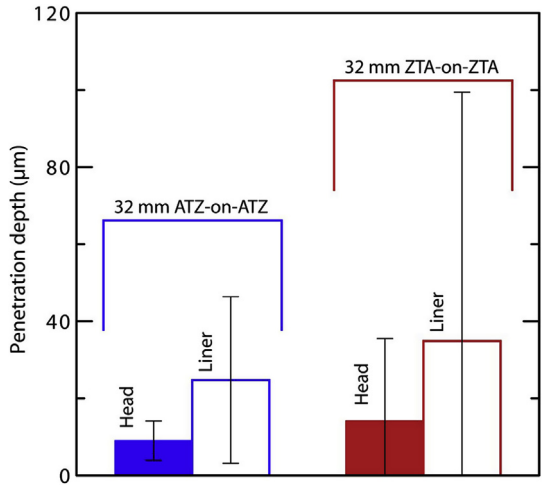

Fig. 5. Maximum penetration depth ± 95% confidence limits of the femoral heads and acetabular liners obtained from the CMM measurements.

ATZ-on-ATZ bearings after 6 million cycles of testing under edge loading conditions however the differences were not significant ($p = 0.4$ and $p = 0.6$ for heads and liners respectively, Fig. 5).

Fig. 6 shows the evolution of the monoclinic fraction measured by XRD with the number of wear cycles, in the wear stripe and on the pole of the heads. Vertical lines represent the evolution of monoclinic

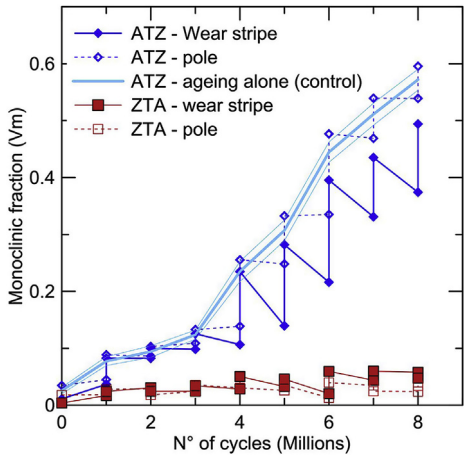

Fig. 6. Monoclinic fraction measured by XRD on ATZ (blue diamonds) and ZTA (red squares) (open symbols: pole; full symbols: wear stripe; no symbol: reference heads submitted to ageing alone (control), the line is surrounded by two thin lines at ± one standard deviation).

fraction during the autoclave time between two series of wear cycles. No significant ageing occurred in the ZTA material. Ageing of ATZ heads was significant and deserved more attention. Three curves are represented on Fig. 6 for ATZ. The dashed one represents ageing of control heads (not subjected to wear, but only to accelerated ageing). The pole of the aged heads followed approximately the same kinetics as the control heads (dotted line with open diamonds) with ageing mainly occurring during the accelerated ageing process. On the wear stripe, each autoclave step increased the monoclinic fraction. However, each one million cycles of wear simulation decreased the monoclinic fraction significantly, resulting in an apparent slower overall ageing kinetics in the wear stripe than at the pole of the heads or in the control heads. However, even if the overall monoclinic fraction evolution was slower in the wear stripe, during autoclave steps the monoclinic fraction increased more in the wear stripe than outside.

This result is confirmed by Fig. 7-a that shows how the depth of the transformed layer in ATZ increased with ageing time. Moreover, this depth slightly decreased during the wear sequences, and the decrease was larger inside the wear stripe than outside. The same analysis was not possible in ZTA (Fig. 7-b) where the scattering of the data was larger than the evolutions from one time-point to another. The depth of the transformed layer seems to be similar for both ceramic materials, i.e. around 1–2 µm.

SEM observations of the worn ATZ and ZTA surfaces showed that the first 2 million cycles (without edge loading) did not significantly damage the surfaces: only few scratches could be observed, and they may originate either from the polishing process or from the wear simulation. Microstructural damage was first observed after 3 million wear cycles (thus after 1 million cycles of edge loading). In ATZ, damage was located in a small wear stripe 15 µm wide, in which the grains were initially blurred (Fig. 8-a and -b). When the number of edge loading cycles increased, the damage remained qualitatively stable, and resulted in grains being pulled out of the surface and the appearance of highly transformed and micro-cracked zirconia grains (Fig. 9-a and -b), while outside of the wear track there was no detectable damage (Fig. 9-c).

In ZTA, damage was first located in a much more diffuse area around 50 µm wide (Fig. 8-c), in which some grains were pulled out and alumina grains were fractured (Fig. 8-d). The same damage characteristics were observed for longer wear times but the width of the wear stripe became larger and the damage density increased: more alumina grains were fractured. This happened seemingly along the basal plane, since all micro-cracks in one grain were parallel to each other, while their orientation differed from grain to grain (Fig. 9-d). The zirconia grains were highly transformed on the surface and in the few remaining agglomerates (Fig. 9-e). Once again, the area outside the wear stripe was not damaged (Fig. 9-f).

Raman maps confirm that in ZTA, the damage was primarily located in alumina grains around the edge of the wear stripe (Fig. 10) that

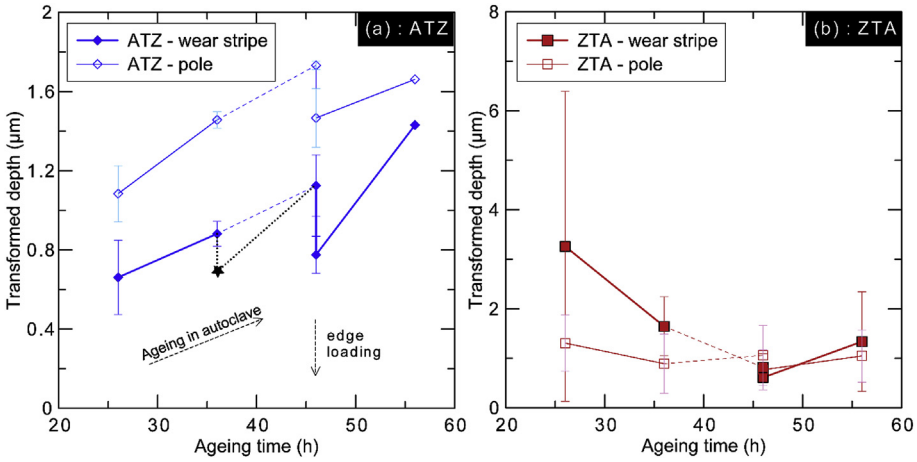

Fig. 7. Evolution of the depth of the transformed surface layer in the wear stripe (track) measured by Raman spectroscopy; (a): ATZ; b): ZTA; (depth shown here are averaged on 5 to 9 profiles measured on a single head per material (the same for each time point; the error bars represent one standard deviation calculated from the same profiles). Dashed lines were used where there is a missing point. Dotted lines and star show a schematic of the expected behaviour (same behaviour is expected for both materials on both locations).

showed a slight decrease of alumina content (calculated with eq. (4) inside the wear stripe, probably indicating pull-out of the most damaged alumina grains.

4. Discussion

It has been shown that the damage of ceramic components increased by the symbiotic combination of ageing, wear and edge loading (Gremillard et al., 2013; Perrichon et al., 2017). However, one must keep in mind that the test proposed here is rather severe, for at least two reasons: first, it simulates edge-loading driven by separation due to suboptimal implant positioning; second, the ageing conditions are also exaggerated, mainly for ATZ (10 h of accelerated ageing after every million wear-cycle, corresponding to 7 years ageing *in vivo* for a number of gait cycles that represent less than 1 year of walking). Based on the data available on similar materials (Chevalier et al., 1999, 2009) at the start of the study, an activation energy of 100–108 kJ mol^{-1} was considered for both materials. With this activation energy, the same monoclinic fraction should be reached with a treatment of 1 h in autoclave at 134 °C, and with a treatment of 1.2–2.5 years at 37 °C (*in vivo* conditions).

Comparing non-worn and worn ATZ, it is clear that wear without edge loading has almost no effect on ageing, since the ageing kinetics were approximately identical on the pole of the heads (where no edge loading contact occurred) and on non-worn (aged-alone) heads. However, the influence of edge loading on ageing was significant: within the wear stripe area, each autoclave step increased the monoclinic fraction, while each million cycles of wear simulation decreased it significantly, resulting in an overall ageing kinetics apparently slower within the wear stripe than at the pole of the heads or on the control heads. Moreover, even if the overall ageing kinetics was slower within the wear stripe, during the autoclave steps, the monoclinic fraction increased more within the wear stripe area than outside (Fig. 6). This behaviour is a strong indication that the monoclinic phase was being

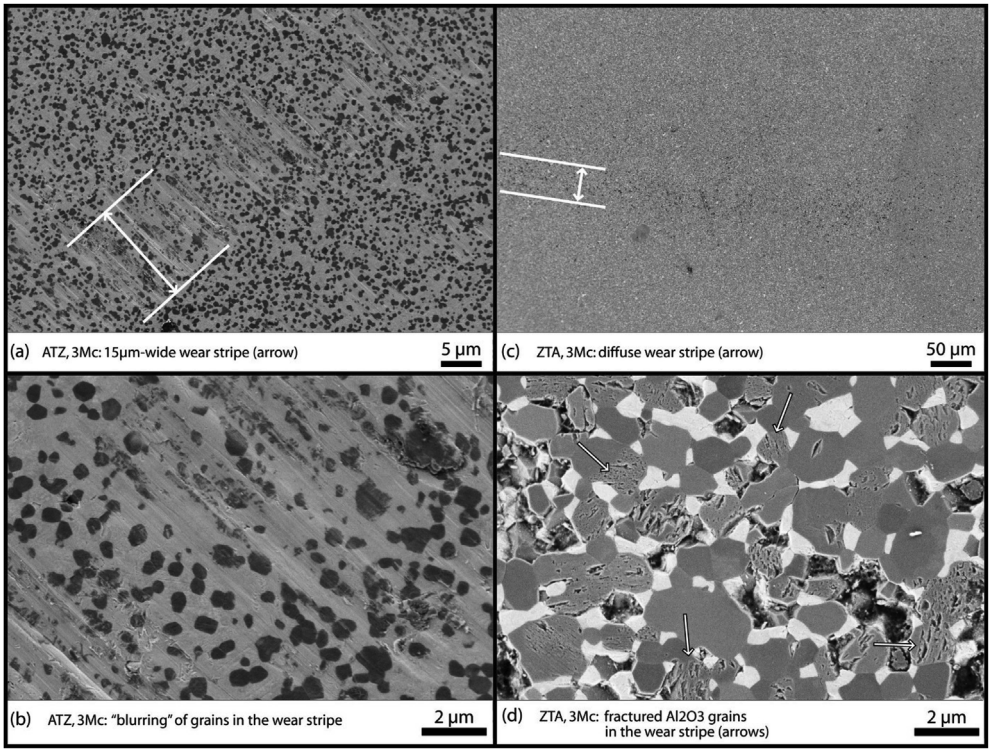

Fig. 8. SEM observation of the initiation of the microstructural damage, after 3 million wear cycles (1 million edge loading cycles) in ATZ ((a) and (b)) and in ZTA ((c) and (d)). (for better clarity, images were submitted to minor gamma and contrast optimisation and sharpening).

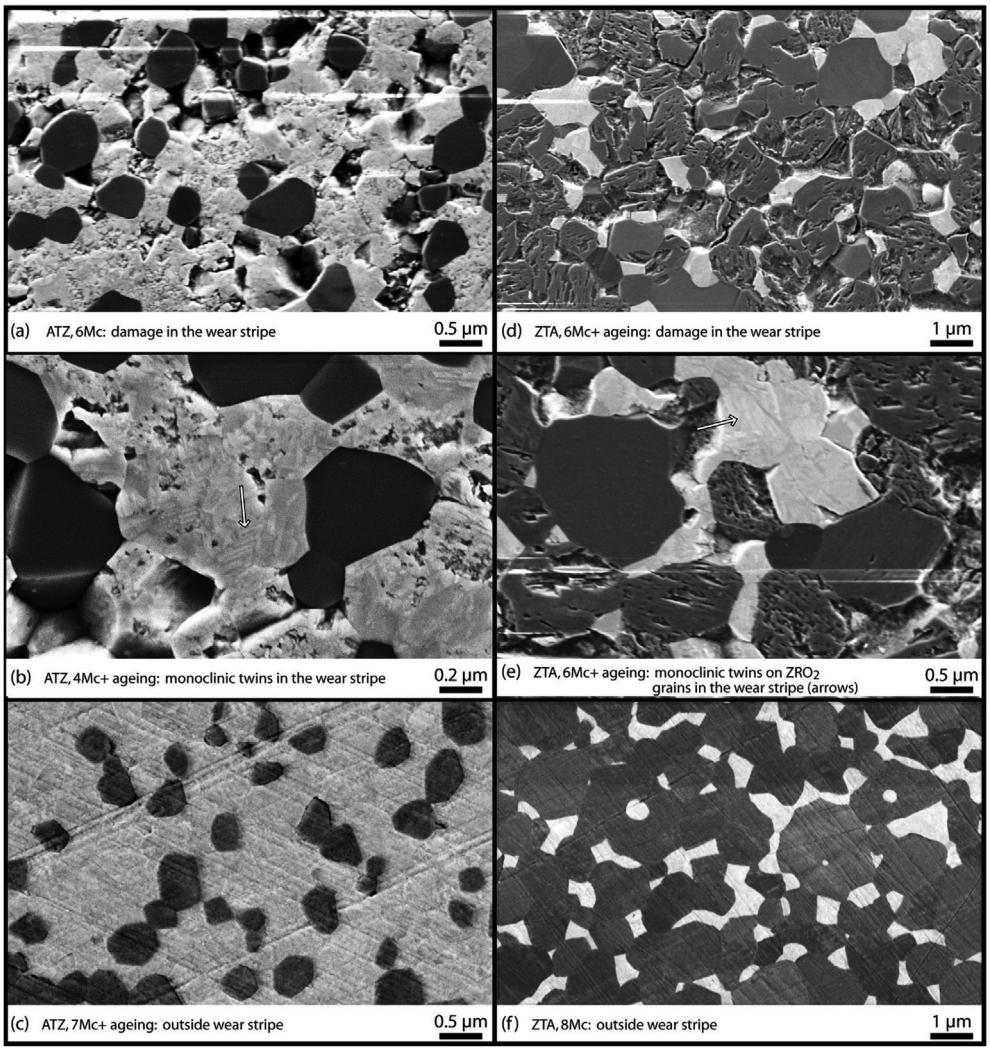

Fig. 9. SEM observations of the microstructure of ATZ ((a), (b), (c)) and ZTA ((d), (e), (f)); (a) and (d) are general views of the wear stripe; (b) and (e) are details in the wear stripe showing monoclinic laths and twins after ageing; (c) and (f) are general views outside the wear stripe, showing undamaged material.(for better clarity, images were submitted to minor gamma and contrast optimisation and sharpening).

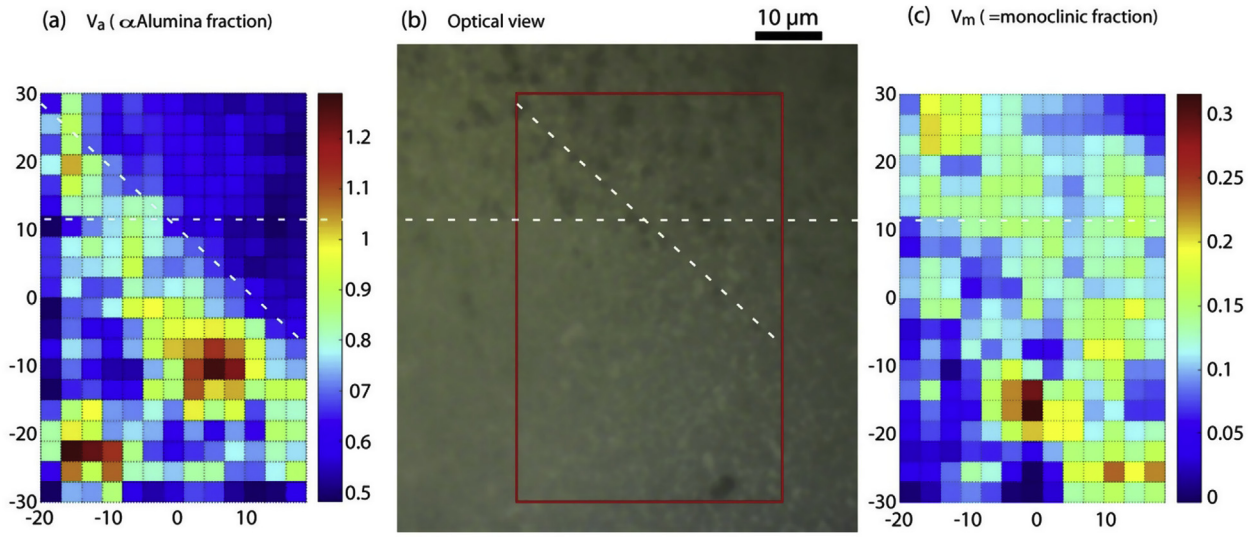

Fig. 10. a- Raman map of V_a (proportional to alumina content) around the edge of the wear stripe in ZTA (scales in μm), b-corresponding optical microscopy view, and c-monoclinic fraction map. Dashed lines are guides for the eyes.

preferentially removed during shocks induced by edge loading. This dependency of the ageing kinetics on the residual stresses resulting from wear or shocks was already observed in previous studies (Gremillard et al., 2013; Perrichon et al., 2017; Douillard et al., 2012).

In ZTA, the monoclinic fractions remained very low over both the wear stripe and the unworn surface, and their variations were within the error margin of XRD. Hence, such a comparison was not possible using XRD as a detection method. However, both SEM observations (Fig. 9) and Raman mapping (Fig. 10) showed that the damage was mainly located in the alumina grains but not in the monoclinic-zirconia grains for ATZ. In both cases, the phase under the highest compressive residual stresses seemed to be the most prone to microstructural damage.

For comparison purposes, SEM images and XRD analysis were also performed on ATZ and ZTA femoral heads tested under edge loading only, for 4 million cycles, without the accelerated ageing process, retrieved from another study (Al-Hajjar et al., 2013b). On these heads the wear rate was 0.14 mm^3 per million cycles, comparable to the present study. The heads presented roughly the same pattern of damage (no damage outside the wear track; in ZTA, damage located in the alumina phase, in ATZ damage located in the zirconia phase). However, the monoclinic fraction was much lower (below 5% for both materials, in all locations on the heads). This highlights the necessity to combine accelerated ageing of the ceramic components with hip simulation to reveal the ageing/wear symbiosis.

One of the limitations of this study was the small number of samples investigated, resulting in a low power of statistics (power 0.4), and exposing the results to statistical accidents such as the behaviour of bearing couple ZTA-ZTA 3. This was also reflected by the difficulty to distinguish statistically significant differences in the wear volumes and penetration depths of ZTA and ATZ (Figs. 3 and 5), and to quantify correctly the evolution of the monoclinic phase on ZTA (Fig. 6). Nevertheless, the mean wear rates of aged ATZ-on-ATZ and ZTA-on-ZTA materials over six million cycles of edge loading wear simulation conditions were relatively low wear at 0.07 mm^3/million cycles and 0.19 mm^3/million cycles respectively.

A second limitation comes from multiple uncertainties regarding the activation energy of ageing. First, very limited data were available at the beginning of the present study, thus activation energy of ageing for both materials was first assumed to be in the range of 100–108 kJ mol^{-1}. However, it was found later that the activation energies were much lower, and different from one material to another: 95.3 kJ mol^{-1} for ATZ, 52 kJ mol^{-1} for ZTA (Gremillard et al., 2018). As a result, it is stipulated that 1 h ageing in autoclave, in water vapour at 134 °C (usual ageing conditions) is equivalent to 0.8 years (9 months and 1 week) ageing at 37 °C for ATZ, and about 5 days for ZTA. It should be noted, as found in (Gremillard et al., 2018), that the overall amount of transformed zirconia (saturation) in ZTA is very low (~2% of the total material) and that the activation barrier is small, which means the ageing starts early but the ongoing is quite slow (see time-temperature equivalence, eq. (1)): 1 year *in vivo* corresponds to 80 h in autoclave, whereas 1 year *in vivo* of ATZ corresponds to only 1.3 h in autoclave. Second, since ageing of ZTA is very slow, it is difficult to measure its activation energy accurately (the same does not apply to ATZ); besides, the very small activation energy measured in (Gremillard et al., 2018) might hint that the slow tetragonal-to-monoclinic phase transformation observed in ZTA does not proceed from the same mechanism than the faster ageing observed in ATZ. Third, it is now known that ageing kinetics are influenced by external factors such as surface finish, residual and applied stresses, and the chemical properties of the environment. However, none of these effects have been fully quantified yet. Thus, the time-temperature dependency of ageing used here (1 h at 134 °C to represent ~9 months for ATZ and 5 days for ZTA), that applies for ageing in steam with no applied stresses, may not be the best assumptions under edge loading conditions. ATZ, with higher amount of monoclinic phase, may be more sensitive to this discrepancy. However, since edge-loading removes the monoclinic phase in ATZ, and ageing was exaggerated during the tests, the uncertainty with regards to the activation energy should not affect the overall ageing behaviour.

The main strength of the study is the combination of edge loading conditions and hydrothermal ageing showing for the first time the symbiotic effect of these two clinically relevant mechanisms. A second strength of the study is the thorough analysis of the changes occurring during wear and ageing within the top layer of the two selected ceramic materials. This allowed the evaluation of the wear mechanics of the ceramic materials throughout the study while re-establishing the material transformation induced by the accelerated ageing.

This study focusses on the most detrimental damage mechanisms during gait (edge loading) combined with the material degradation effects of ageing, and to the author's knowledge is the first study to do so. It provides an indication of the potential state of ceramic hip joint components after longer term *in vivo* use. Recent analysis of clinical retrievals has predominantly focused on failure due to fracture, rather than specifically looking for evidence of edge loading and/or material degradation. However, the sensitivity of hard bearings to proper component position and edge loading was emphasized in a study reporting the incidence of modern alumina bearing failures from a single major ceramic manufacturer in nearly 6 million hip implants, where it was shown that smaller ball heads were more likely to fracture (Lee and Kim, 2017).

5. Conclusion

In this study, a method was devised by which the performance of composite ceramic materials was assessed under a combination of edge loading gait conditions and hydrothermal ageing. The damage of ceramic components increased by the symbiotic effect of ageing, wear and shocks but remained at a very low level for both ceramic materials. It was shown that the performance of ATZ-on-ATZ materials *in vitro* may be superior to ZTA-on-ZTA materials despite the higher zirconia content in the ATZ materials. In conclusion, ceramics composites such as ATZ-on-ATZ and ZTA-on-ZTA have shown the potential to provide low wear material solutions in hip replacement.

Acknowledgement

This study was funded by Mathys Orthopädie GmbH, Moersdorf, Germany, EPSRC Centre for Innovative Manufacturing in Medical Devices (MeDe Innovation; grant number EP/K029592/1) and by the Federal Ministry of Education and Research of Germany (ref. no. 03WKCB01K).

Appendix A. Supplementary data

Supplementary data to this article can be found online at https://doi.org/10.1016/j.jmbbm.2019.05.011.

References

Al-Hajjar, M., Jennings, L.M., 2019. Data Associated with 'Combined Wear and Ageing of Ceramic-On-Ceramic Bearings in Total Hip Replacement under Edge Loading Conditions'. University of Leeds. https://doi.org/10.5518/593.

Al-Hajjar, M., Leslie, I.J., Tipper, J., Williams, S., Fisher, J., Jennings, L.M., 2010. Effect of cup inclination angle during microseparation and rim loading on the wear of BIOLOX (R) delta ceramic-on-ceramic total hip replacement. J. Biomed. Mater. Res. B Appl. Biomater. 95, 263–268.

Al-Hajjar, M., Fisher, J., Tipper, J.L., Williams, S., Jennings, L.M., 2013a. Wear of 36-mm BIOLOX(R) delta ceramic-on-ceramic bearing in total hip replacements under edge loading conditions. Proc. Inst. Mech. Eng. H 227, 535–542.

Al-Hajjar, M., Jennings, L.M., Begand, S., Oberbach, T., Delfosse, D., Fisher, J., 2013b. Wear of novel ceramic-on-ceramic bearings under adverse and clinically relevant hip simulator conditions. J. Biomed. Mater. Res. B Appl. Biomater. 101, 1456–1462.

Al-Hajjar, M., Carbone, S., Jennings, L.M., Begand, S., Oberbach, T., Delfosse, D., et al., 2017. Wear of composite ceramics in mixed-material combinations in total hip replacement under adverse edge loading conditions. J. Biomed. Mater. Res. B Appl.

Biomater. 105B, 1361–1368.
Barbour, P.S., Stone, M.H., Fisher, J., 1999. A hip joint simulator study using simplified loading and motion cycles generating physiological wear paths and rates. Proc Inst Mech Eng [H] 213, 455–467.
Bierbaum, B.E., Nairus, J., Kuesis, D., Morrison, J.C., Ward, D., 2002. Ceramic-on-ceramic bearings in total hip arthroplasty. Clin. Orthop. Relat. Res. 158–163.
Blumenfeld, T., Glaser, D., Bargar, W., Langston, G., Mahfouz, M.R.K., 2011. In *vivo* assessment of total hip femoral head separation from the acetabular cup during 4 common daily activities. Orthopedics 34, 127–132.
Boutin, P., 1971. Experimental study of aluminium in surgery of hip. Presse Med. 79, 639–640.
Chevalier, J., Cales, B., Drouin, J.M., 1999. Low-temperature aging of Y-TZP ceramics. J. Am. Ceram. Soc. 82, 2150–2154.
Chevalier, J., Grandjean, S., Kuntz, M., Pezzotti, G., 2009. On the kinetics and impact of tetragonal to monoclinic transformation in an alumina/zirconia composite for arthroplasty applications. Biomaterials 30, 5279–5282.
Clarke, D.R., Adar, F., 1982. Measurement of the crystallographically transformed zone produced by fracture in ceramics containing tetragonal zirconia. J. Am. Ceram. Soc. 65, 284–288.
D'Antonio, J.A., Capello, W.N., Naughton, M., 2012. Ceramic bearings for total hip arthroplasty have high survivorship at 10 years. Clin. Orthop. Relat. Res. 470, 373–381.
Dennis DA, Komistek RD, Northcut EJ, Ochoa JA, Hammill C. *In Vivo* Determination of Hip Joint Separation in Subjects Having Either a Metal on Metal or Metal on Polyethylene Total Hip Arthroplasty. 47th Annual Meeting Orthopaedic Research Society. San Francisco2001.
Douillard, T., Chevalier, J., Descamps-Mandine, A., Warner, I., Galais, Y., Whitaker, P., et al., 2012. Comparative ageing behaviour of commercial, unworn and worn 3Y-TZP and zirconia-toughened alumina hip joint heads. J. Eur. Ceram. Soc. 32, 1529–1540.
Garvie, R.C., Nicholson, P.S., 1972. Phase Analysis in zirconia systems. J. Am. Ceram. Soc. 55, 303–305.
Gremillard, L., Martin, L., Zych, L., Crosnier, E., Chevalier, J., Charbouillot, A., et al., 2013. Combining ageing and wear to assess the durability of zirconia-based ceramic heads for total hip arthroplasty. Acta Biomater. 9, 7545–7555.
Gremillard, L., Chevalier, J., Martin, L., Douillard, T., Begand, S., Hans, K., et al., 2018. Sub-surface assessment of hydrothermal ageing in zirconia-containing femoral heads for hip joint applications. Acta Biomater. 68, 286–295.
Kobayashi, K., Kuwajima, H., Masaki, T., 1981. Phase change and mechanical properties of ZrO2-Y2O3 solid electrolyte after ageing. Solid State Ionics 3–4, 489–493.
Lee, G.-C., Kim, R.H., 2017. Incidence of modern alumina ceramic and alumina matrix composite femoral head failures in nearly 6 million hip implants. J. Arthroplast. 32, 546–551.
Leslie, I., Williams, S., Isaac, G., Ingham, E., Fisher, J., 2009. High cup angle and microseparation increase the wear of hip surface replacements. Clin. Orthop. Relat. Res. 467, 2259–2265.
Nevelos, J., Ingham, E., Doyle, C., Streicher, R., Nevelos, A., Walter, W., et al., 2000. Microseparation of the centers of alumina-alumina artificial hip joints during simulator testing produces clinically relevant wear rates and patterns. J. Arthroplast. 15, 793–795.
Perrichon, A., Reynard, B., Gremillard, L., Chevalier, J., Farizon, F., Geringer, J., 2017. A testing protocol combining shocks, hydrothermal ageing and friction, applied to Zirconia Toughened Alumina (ZTA) hip implants. J. Mech. Behav. Biomed. Mater. 65, 600–608.
Petsatodis, G.E., Papadopoulos, P.P., Papavasiliou, K.A., Hatzokos, I.G., Agathangelidis, F.G., Christodoulou, A.G., 2010. Primary cementless total hip arthroplasty with an alumina ceramic-on-ceramic bearing results after a minimum of twenty years of follow-up. J. Bone Joint Surgery-American 92A, 639–644.
Sentuerk, U., Von Roth, P., Perka, C., 2016. Ceramic on ceramic arthroplasty of the hip. The Bone & Joint Journal 98-B, 14–17.
Stewart, T.D., Tipper, J.L., Insley, G., Streicher, R.M., Ingham, E., Fisher, J., 2003a. Long-term wear of ceramic matrix composite materials for hip prostheses under severe swing phase microseparation. J. Biomed. Mater. Res. B Appl. Biomater. 66, 567–573.
Stewart, T.D., Tipper, J.L., Insley, G., Streicher, R.M., Ingham, E., Fisher, J., 2003b. Severe wear and fracture of zirconia heads against alumina inserts in hip simulator studies with microseparation. J. Arthroplast. 18, 726–734.
Toraya, H., Yoshimura, M., Somiya, S., 1984. Calibration curve for quantitative analysis of the monoclinic-tetragonal ZrO2 system by X-ray diffraction. J. Am. Ceram. Soc. 67 C-119, C-21.
Williams, S., Leslie, I., Isaac, G., Jin, Z., Ingham, E., Fisher, J., 2008. Tribology and wear of metal-on-metal hip prostheses: influence of cup angle and head position. J Bone Joint Surg Am 90 (Suppl. 3), 111–117.
Yoon, B.-H., Park, I.K., 2018. Atraumatic fracture of the BIOLOX delta ceramic liner in well-fixed total hip implants. Orthopedics 41 (6), e880–e883.